

# A Definition of Thermophysiological Parameters of SAM Materials for Temperature Rise Calculation in the Head of Cellular Handset User

S. I. Al-Mously<sup>1</sup> and M. M. Abousetta<sup>2</sup>

<sup>1</sup>Department of Electrical and Computer Engineering

School of Applied Sciences and Engineering, Academy of Graduate Studies, Tripoli, Libya

<sup>2</sup>Department of Electrical and Electronics Engineering, Faculty of Engineering  
Al-Fateh University, Tripoli, Libya

**Abstract**— A definition of thermophysiological parameters of the Specific Anthropomorphic Mannequin (SAM) CAD model material is proposed in this paper to calculate the temperature-rise in the head of cellular handset users. The SAM materials have the electrical and thermal parameters based on the averaged properties of a heterogeneous High-Resolution European Female Head (HR-EFH) with twenty five different tissues. The specific absorption rate (SAR) and the temperature-rise in the SAM because of the exposure to radiation of different handset models, i.e., candy-bar with external antenna and candy-bar with internal antenna, are calculated in the GSM900 and GSM1800 using a FDTD-based platform. The computations were also carried out applying HR-EFH for comparison.

## 1. INTRODUCTION

Since the biological hazards due to RF exposure in cellular communications are caused mainly by a temperature-rise in tissue, calculations of temperature may be preferable to calculations of SAR because of the more direct relationship between temperature and safety. Thus, the effect of localized SAR for portable telephones should also be related to the temperature-rise in the human head.

The temperature increase in the anatomically based human head models due to handset antennas has been calculated in quite a few works, as in [1–3]. In those works, the handset is simulated using either dipole antenna or monopole over a rectangular metal box (dielectric covered or none-covered) or a simple metal chassis with shorted-patch antenna. None of the previous work has considered a realistic or semi-realistic handset models in evaluating their thermal effect on tissues, as considered in this paper.

In this paper, the bioheat equation is solved using a Finite-Difference Time-Domain (FDTD)-based Electromagnetic (EM) solver, *SEMCAD X* [4], to compute the temperature-rise in both anatomically based human head and SAM as related to, first, the antenna radiated power of 0.6 W at 900 MHz and 0.125 W at 1800 MHz, second, safety SAR limits [5, 6].

## 2. PENNES BIOHEAT EQUATION (BHE)

Temperature ( $T = T(x, y, z, t)$  [°C]) was modeled in the head with a finite difference implementation of bioheat transfer equation (BHE), developed by Pennes in 1948 [7]:

$$\rho c \frac{\partial T}{\partial t} = \nabla \cdot (k \nabla T) + \rho Q_{met} + \rho(\text{SAR}) - B(T - T_{blood}) \quad (1)$$

$$B = \rho_{blood} c_{blood} \rho \omega \quad (2)$$

where the  $\rho$  [kg/m<sup>3</sup>] is the material density,  $c$  [J/(kg · °C)] is the specific heat capacity,  $k$  [W/(m · °C)] is the thermal conductivity,  $Q_{met}$  [W/kg] is the metabolic heat generation rate,  $B$  [W/(m<sup>3</sup> · °C)] is the blood perfusion coefficient,  $\omega$  [L/(s · kg)] is the blood perfusion rate, and  $T_{blood}$  is blood temperature. In (1), the term on the left represents the rate of change in the stored internal energy of the tissue, the term  $\nabla \cdot (k \nabla T) = k \nabla^2 T$  is the heat transfer due to thermal conduction, and the last term relates convection heat loss associated with blood flow. The heat is distributed through the simulation domain by diffusion. It is generated by metabolic body processes and by the deposited radiation energy. A homogeneous ‘heat-sink’ term has a cooling effect and models the heat removal due to blood circulation.

Heat exchange at the tissue interface with the surrounding environment is modeled by imposing the continuity of heat flow perpendicular to the skin surface as the boundary condition. Various

boundary conditions are commonly applied: the Dirichlet ( $T = T_a$ ), the Neumann ( $k\partial T/\partial n = q$ ) and the mixed boundary condition which is used and expressed as;

$$k\frac{\partial T}{\partial n}(x, y, z) = -H_a(T_{skin} - T_a) \left[ \frac{W}{m^2} \right] \quad (3)$$

where  $n$  is the normal to the skin surface and the right hand expression models the heat losses from surface of the skin due to convection and radiation which are proportional to the difference between the skin temperature ( $T_{skin}$ ) and external environment (ambient) temperature ( $T_a$ ),  $H_a$  is the convection coefficient for heat exchange with the external temperature. In this study, the heating due to RF absorption is very small; therefore, the neglecting of sweating does not make any difference.

### 3. TEMPERATURE-RISE CALCULATION IN HETEROGENEOUS HEAD MODEL

The temperature-rise in HR-EFH due to handheld set model-A (candy-bar type with external top-loaded short whip antenna) and Model-B (candy-bar type with internal short patch antenna) [8] while in use has been computed at 900 and 1800 MHz. Figure 1 shows both handset models with realistic hand-holding and close to head (HR-EFH and SAM) at *cheek*-position. The tissues electrical properties given in [8] and the thermal properties given in Table 1 are used.

Solving the BHE using the conformal-FDTD method to compute the temperature-rise in handset user's head due to the SAR deposition needs accomplishing two simulations; first, the EM-simulation to compute the deposited SAR in tissue, second, thermo-simulation to compute the temperature-rise in tissue. In the EM-simulation achieved in this paper, the FDTD-grid for each handset setup has a minimum spatial resolution of  $0.5 \times 0.5 \times 0.5 \text{ mm}^3$  and maximum resolution of  $10 \times 10 \times 10 \text{ mm}^3$  in the  $x$ ,  $y$ , and  $z$  directions with grading ratio of 1.2. The absorbing boundary conditions (ABCs) are set as U-PML mode with 10 layers thickness [4]. This FDTD-grid setting is also applied in thermo-simulation. A mixed boundary condition given in (3) involving skin plus ears is used with convection coefficient ( $H_a = 2.7 \text{ W}/(\text{m}^2 \text{ }^\circ\text{C})$ ) and ambient temperature ( $T_a = 25^\circ\text{C}$ ). The core temperature is ( $T_{blood} = 37^\circ\text{C}$ ). The heat exchanged through the neck and the other remaining parts of the body has been approximated by means of setting the neck boundary temperature as the blood temperature.

It should be noticed that the results based on experiments involving animals are used for most of the thermal parameters required in the human-head model [2]. Since no solid relations describing the thermal parameters dependency on the minor expected temperature-rise in head of the handset user; in this paper, blood perfusion coefficient is modeled to be linearly temperature dependent as based on the temperature distribution and blood perfusion response in rat brain during selective brain cooling presented by Diao and Zhu in [9]. Although the heat dissipation in the skin of rats differs from that of in the human skin, the experiment results presented in [9] are used to approximate per  $1^\circ\text{C}$  blood perfusion in brain, skin and ears tissue at a rate value of 13%, while computing the temperature-rise in the head of handset user.

Table 2 depicts the number of generated voxels, the computed SAR(1g) induced in HR-EFH

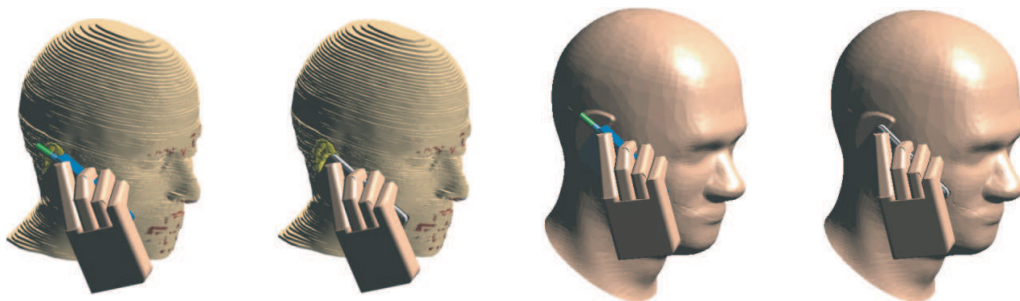


Figure 1: Handset models-A and B setups for temperature-rise computation in HR-EFH as well as in SAM. (a) Handheld set model-A at *cheek*-position with HREFH. (b) Handheld set model-B at *cheek*-position with HREFH. (c) Handheld set model-A at *cheek*-position with SAM. (d) Handheld set model-B at *cheek*-position with SAM.

Table 1: Mass, mass density and thermal properties assumed for the various HR-EFH tissues [1–3].

HR-EFH Tissue	Mass	$\rho$ [kg/m <sup>3</sup> ]	$c$ [J/(kg · °C)]	$k$ W/(m · °C)]	$Q_{met}$ [W/kg]	$B$ [W/(m <sup>3</sup> · °C)]
1. Air	0.000	1.16	1006	0.0263	0	0
2. Blood Vessel	0.005	1050	3553	0.46	1.52	1000
3. Bone	0.030	1990	1300	0.4	0.15	1000
4. Brain /grey matter	0.871	1039	3700	0.57	9.7	35000
5. Brain /white matter	0.367	1043	3600	0.5	9.7	35000
6. Cerebellum	0.125	1040	4200	0.58	9.7	35000
7. CSF	0.256	1007	4000	0.6	0	0
8. Ear (cartilage)	0.011	1100	3400	0.45	0.2	9100
9. Eye-cornea	0.002	1032	4200	0.58	0.0	0.0
10. Eye-lens	0.002	1090	3000	0.4	0.0	0.0
11. Eye-vitreous body	0.010	1009	4200	0.6	0.34	0
12. Fat	0.032	916	2500	0.25	0.15	520
13. Jaw bone	0.243	1990	1300	0.4	0.15	1000
14. Mastoid cells	0.027	980	2700	0.22	5.82	32000
15. Mid-brain	0.026	1039	3700	0.57	9.7	35000
16. Muscles	0.940	1041	3600	0.5	0.67	2700
17. Nasal cavity	0.063	1050	3300	0.43	1.523	9000
18. Parotid Gland	0.020	1050	3700	0.53	9.7	25000
19. Skin/dermis	0.760	1100	3500	0.42	1.07	9100
20. Skull	0.744	1645	1300	0.4	0.15	1000
21. Spinal cord	0.007	1038	3500	0.46	9.7	35000
22. Spine	0.120	1990	1300	0.4	0.15	1000
23. Thalamus	0.015	1039	3700	0.57	9.7	35000
24. Tongue	0.035	1041	3300	0.42	0.461	13000
25. Ventricles (brain)	0.005	1007	4200	0.6	0	0

Table 2: Number of the generated voxels, peak SAR (1 g) induced in whole HR-EFH and in brain, and the corresponding peak temperature-rise after 60 min of using the handheld set models-A and B with antenna output power of 600 mW at 900 MHz and 125 mW at 1800 MHz.

900 MHz	Position	No. of Voxels	SAR <sub>1g</sub> in Head (W/kg)	SAR <sub>1g</sub> in Brain (W/kg)	Max. $T$ in Head (°C)	Max. $T$ in Brain (°C)
Model-A	Cheek	23409725	4.70	2.08	37.43	37.28
	Tilt	22581248	3.70	1.85	37.35	37.25
Model-B	Cheek	24175264	3.88	0.82	37.45	37.26
	Tilt	24226455	2.26	0.62	37.34	37.19
1800 MHz	Position	No. of Voxels	SAR <sub>1g</sub> in Head (W/kg)	SAR <sub>1g</sub> in Brain (W/kg)	Max. $T$ in Head (°C)	Max. $T$ in Brain (°C)
Model-A	Cheek	23955708	1.63	0.51	37.31	37.20
	Tilt	24147585	1.62	0.61	37.32	37.21
Model-B	Cheek	24420000	1.60	0.24	37.30	37.14
	Tilt	24680656	1.39	0.23	37.28	37.13

tissues and in brain, i.e., ventricles, thalamus, spinal cord, mid-brain, cerebro spinal fluid, cerebellum, grey matter and white matter, and their corresponding steady-state temperature after 60 min of using the handheld set models-A and B and normalized to antenna radiated power of 600 mW at

900 MHz and 125 mW at 1800 MHz. The 600 mW antenna radiated power is for the analogue phone, whereas, the radiated power of digital generation of GSM mobile phone is 250 mW at 900 MHz. That is because the main aim of the study is to calculate the maximum temperature-rise in human head due to the possible maximum RF emission for the purpose of comparison with previously published works on this subject.

Although the IEEE [5] and FCC [6] standards apply the SAR limit for the extremities to the normal pinnae, and since the used MRI-based head model (HR-EFH) has pressed pinnae; in this paper, the pinnae are subject to the same exposure limit, for peak spatial SAR, as the head. It has been observed that there are no substantial differences between the computed SAR values for the head with and without pressed pinnae, where the peak spatial SAR location is not at the pinna, instead the peak shift to region near the pinna.

The results show that the global maximum field position of both SAR and its corresponding temperature are not identical; while the peak SAR occurs outside the pinna or skin surfaces depending on the handset position, the peak temperature occurs inside the head tissues and mostly in cheek muscle. Moreover, the handset position plays an important role in convection. For the same SAR values, the handset at *cheek*-position induces more temperature in head than handset at *tilt*-position, and this behavior increased while using handheld set model-B, as compared with handheld set model-A. Positioning the handset close to head at *cheek*-position, first, moves the peak SAR position from the pinna to cheek skin, second, blocks the convective heat exchange between the skin layers and air, causing temperature rises in the tissues around the contact zone.

The computed possible temperature-rise in head and brain (using HR-EFH) for the SAR prescribed in the safety IEEE [5] and FCC [6] standards are  $0.3 \pm 0.02$  and  $0.16 \pm 0.02$ , respectively, for the different handset models in different conditions. These results are coinciding with that given in [2].

Simulating the heated-handset with a temperature of  $39^\circ\text{C}$ , which measured practically for different commercial cellular handsets, temperatures of  $38.36^\circ\text{C}$  and  $38.48^\circ\text{C}$  are noticed in the ear tissue for the handset model-A at *cheek* and *tilt*-position, respectively, whereas, temperatures of  $38.86^\circ\text{C}$  and  $38.85^\circ\text{C}$  are noticed in the ear tissue for the handset model-B at *cheek* and *tilt*-position, respectively, but without any considerable temperature increase in the brain tissue. These results are agreed with that given in [1].

Table 3: The proposed dielectric and thermal parameters of the SAM phantom materials computed using (4). Mass density of the shell =  $1100 \text{ kg/m}^3$  and mass density of inside-material =  $1000 \text{ kg/m}^3$ .

SAM material	Frequency	$\epsilon_r$	$\sigma$ [S/m]	$c$ [J/(kg · °C)]	$k$ [W/(m · °C)]	$Q_{met}$ [W/kg]	$B$ [W/(m <sup>3</sup> · °C)]
Shell	900 MHz	41.41	0.87	3500	0.42	1.07	9100
	1800 MHz	38.87	1.18				
Inside	900 MHz	41.30	0.79	2982.7	0.49	3.79	14050
	1800 MHz	39.60	1.13				

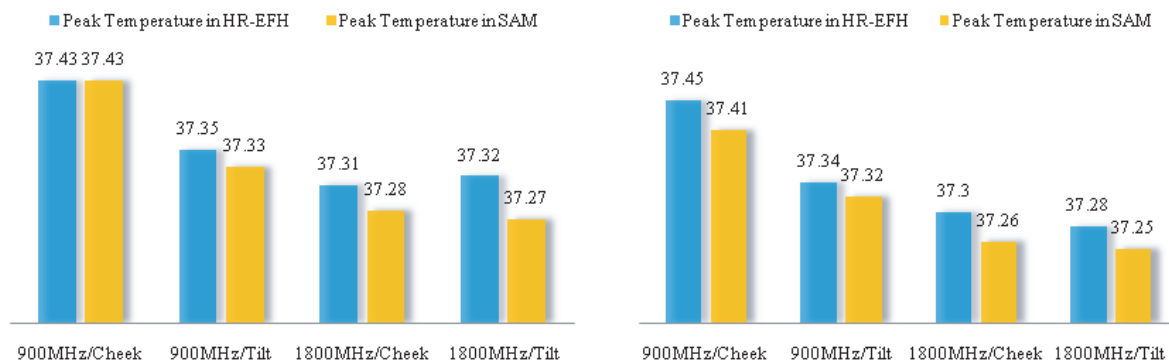


Figure 2: Peak temperature values ( $^\circ\text{C}$ ) corresponding to the spatial peak SAR(1g) values induced in HR-EFH and SAM whole phantom given in Tables 2 and 3 due to; (a) Handheld set model-A and (b) Handheld set model-B, in different conditions.

#### 4. TEMPERATURE-RISE CALCULATION IN SAM

It is essential to have a standard phantom with standard thermophysiological parameters to simulate the temperature-rise in the entire head of cellular handset users, as many anatomically correct head models are available for different sexes, ages, resolutions and number of tissues; with different parameters, which as a result give different temperature-rise induced by cellular handsets [2].

Both pinnae are a part of the shell in the SAM phantom and are not tissue-simulating materials. In order to simulate a real pressed ear, which may play an important role in simulating the temperature-rise in human head due to the RF emission of mobile phone, a definition of thermophysiological parameters of SAM CAD-phantom materials is proposed as follows; the entire shell has the electrical and thermal properties similar to that of HR-EFH skin-tissue, whereas, the lossy inside-material has the electrical and thermal parameters based on the averaged properties of the HR-EFH tissues (excluding skin and cartilage tissues). The electrical and thermal parameters of the 23 different HR-EFH tissues are averaged using the following equation, and considered as the SAM inside-material parameters, Table 3.

$$SAM \text{ Parameter}(n) = \sum_{i=1}^{23} \text{parameter}(n) \text{ of HR-EFH tissue}(i) \cdot \frac{\text{Mass of tissue}(i)}{\text{Head total mass}} \quad (4)$$

Parameter ( $n = 1, 2, 3, 4, 5$  and  $6$ )  $\equiv \epsilon_r, \sigma, c, k, Q_{met}$  and  $B$ , respectively.  $\epsilon_r$  and  $\sigma$  are frequency dependent.

Using the thermophysiological parameters given in Table 3, the steady-state temperature in SAM materials due to handheld set models-A and B are computed in different conditions, Figure 2.

#### 5. CONCLUSION

The definition of the thermophysiological parameters of the SAM material proposed in this paper show a temperature-rise in head due to the cellular handset comparable to that calculated using an MRI-based heterogeneous head model. Thus, these parameters definition may be applied numerically using SAM phantom to standardize the temperature-rise simulation in the head of cellular handset users.

#### REFERENCES

1. Bernardi, P., M. Cavagnaro, S. Pisa, and E. Piuzzi, "Power absorption and temperature elevations induced in the human head by a dual-band monopole-helix antenna phone," *IEEE Transaction on Microwave Theory and Techniques*, Vol. 49, No. 12, 1118–1126, Dec. 2001.
2. Hirata, A. and T. Shiozawa, "Correlation of maximum temperature increase and peak SAR in the human head due to handset antennas," *IEEE Transaction on Microwave theory and Techniques*, Vol. 51, No. 7, 1834–1841, Jul. 2003.
3. Fujimoto, M., A. Hirata, J. Wang, O. Fujiwara, and T. Shiozawa, "FDTD-derived correlation of maximum temperature increase and peak SAR in child and adult head models due to dipole antenna," *IEEE Transactions on Electromagnetic Compatibility*, Vol. 48, No. 1, 240–247, Feb. 2006.
4. SEMCAD, X, "Reference manual for the SEMCAD simulation platform for electromagnetic compatibility, antenna design and dosimetry," *SPEAG-Schmid & Partner Engineering AG*, <http://www.semcad.com>.
5. "Standard for Safety levels with respect to human exposure to radiofrequency electromagnetic fields, 3 kHz to 300 GHz," *IEEE Standards Coordinating Committee*, 28.4, 2006.
6. "Evaluating compliance with FCC guidelines for human exposure to radio frequency electromagnetic field, supplement C to OET bulletin 65," *Federal Communications Commission*, Edition 9701, Washington, DC, USA, 1997.
7. Pennes, H. H., "Analysis of tissue and arterial blood temperature in resting forearm," *J. Appl. Phys.*, Vol. 1, 93–122, 1948.
8. Al-Mously, S. I. and M. M. Abousetta, "Anticipated impact of hand-hold position on the electromagnetic interaction of different antenna types/positions and a human in cellular communications," *International Journal of Antennas and Propagation*, Vol. 2008, Article ID 102759, 22, 2008.
9. Diao, C. and L. Zhu, "Temperature distribution and blood perfusion response in rat brain during selective brain cooling," *Med. Phys.*, Vol. 33, No. 7, 2565–2573, Jul. 2006.